

A new species of the blind and miniature genus *Micromyzon* Friel and Lundberg, 1996 (Siluriformes: Aspredinidae) from the Orinoco River: describing catfish diversity using high-resolution computed tomography

Author(s): Tiago P. Carvalho, John G. Lundberg, Jonathan N. Baskin, John P. Friel, Roberto E. Reis

Source: Proceedings of the Academy of Natural Sciences of Philadelphia, 165(1):37-53.

Published By: The Academy of Natural Sciences of Philadelphia

<https://doi.org/10.1635/053.165.0104>

URL: <http://www.bioone.org/doi/full/10.1635/053.165.0104>

BioOne (www.bioone.org) is a nonprofit, online aggregation of core research in the biological, ecological, and environmental sciences. BioOne provides a sustainable online platform for over 170 journals and books published by nonprofit societies, associations, museums, institutions, and presses.

Your use of this PDF, the BioOne Web site, and all posted and associated content indicates your acceptance of BioOne's Terms of Use, available at www.bioone.org/page/terms_of_use.

Usage of BioOne content is strictly limited to personal, educational, and non-commercial use. Commercial inquiries or rights and permissions requests should be directed to the individual publisher as copyright holder.

A new species of the blind and miniature genus *Micromyzon* Friel and Lundberg, 1996 (Siluriformes: Aspredinidae) from the Orinoco River: describing catfish diversity using high-resolution computed tomography

TIAGO P. CARVALHO

Laboratório de Ictiologia, Departamento de Zoologia, Universidade Federal do Rio Grande do Sul. Av. Bento Gonçalves, 9500, 91501-970 Porto Alegre, RS, Brazil

Department of Ichthyology, The Academy of Natural Sciences, 1900 Benjamin Franklin Parkway, 19103-1195 Philadelphia, PA, USA
E-mail: carvalho.ictio@gmail.com

JOHN G. LUNDBERG

Department of Ichthyology, The Academy of Natural Sciences, 1900 Benjamin Franklin Parkway, 19103-1195 Philadelphia, PA, USA
E-mail: lundberg@ansp.org

JONATHAN N. BASKIN

Emeritus Professor, Biological Sciences Department, California State Polytechnic University, 91768, Pomona, CA, USA
Research Associate, Los Angeles County Museum of Natural History, 900 Exposition Blvd, 90007 Los Angeles, CA, USA
Email: jnbaskin@gmail.com

JOHN P. FRIEL

Alabama Museum of Natural History, The University of Alabama, Box 870340, Tuscaloosa, AL, 35487-0340, USA.
Email: jpfriel@ua.edu

ROBERTO E. REIS

PUCRS, Laboratory of Vertebrate Systematics. P. O. Box 1429, 90619-900 Porto Alegre, RS, Brazil.
Email: reis@pucrs.br

ABSTRACT.—A new species of the aspredinid catfish tribe *Hoplomyzontini* *Micromyzon* is described from two specimens collected with trawl nets in two localities, at 10 and 18 m depth, in the main channel of the lower Orinoco River in Venezuela almost 40 years ago. The new species is distinguished from its only congener, *Micromyzon akamai*, by the: straight anterior margin of the mesethmoid; open posterior cranial fontanel; ossified first pectoral-fin radial; single tubular infraorbital bone; infraorbital sensory canal entering neurocranium via the frontal; enclosed foramen for the *abductor superficialis* muscle in the coracoid; higher vertebral count (33 vs. 28–32); higher anal-fin ray count (10 or 11 vs. 7–9); and some morphometric features. The holotype of the new species was scanned using High-Resolution X-ray Computed Tomography to illustrate, describe, and compare its bony skeleton to other *Hoplomyzontini*.

RESUMEN.—Una nueva especie de *Hoplomyzontini* *Micromyzon* se describe a partir de dos muestras colectadas con redes de arrastre en dos localidades, entre 10 y 18 metros de profundidad, en el canal principal de la parte baja del Río Orinoco, en Venezuela hace casi 40 años. La nueva especie se diagnostica de su único congénere, *Micromyzon akamai*, por la margen anterior recta del mesetemoide; parte posterior de la fontanela craneal abierta; el primer radial de la aleta pectoral osificado, un solo hueso infraorbital tubular; el canal sensorial infraorbital entra al neurocráneo a través del frontal; un foramen cerrado para el musculo *abductor superficialis* en el e coracoide; mayor número de vértebras (33 vs. 28–32) y del número de radios anales (10 o 11 vs. 7–9); además de algunas características morfológicas. El holotipo de la nueva especie fue escaneado en alta resolución utilizando Tomografía Computarizada de Radio-X de Alta Resolución, y se describe su osteología y se compara con otros *Hoplomyzontini*.

Keywords: Anophthalmic, Miniaturization, Neotropical, River Channels, Taxonomy

Submission Date: November 2, 2016 Acceptance Date: December 14, 2016 Publication Date: December 29, 2016

INTRODUCTION

The genus *Micromyzon* belongs to the Aspredinidae, a moderately diverse South American family of catfishes that contains 45 valid species distributed in 13 genera (Friel, 2003; Eschemeyer and Fong, 2016; Friel and Carvalho, 2016; Carvalho et al., in press a,b). *Micromyzon* is also included within the aspredinid tribe Hoplomyzontini, a peculiar group characterized by small body size, body armor formed by dorsal and ventral vertebral processes, and expanded lateral-line ossicles (Fernández-Yepéz, 1953; Taphorn and Marrero, 1990; Friel and Lundberg, 1996). Most hoplomyzontins are distributed in the western Amazon, western Orinoco, Maracaibo and Magdalena river drainages at elevations between 50 and 600 m asl in the Andean piedmont (Taphorn and Marrero, 1990; Maldonado-Ocampo et al., 2005). Heretofore, records of Hoplomyzontini outside this region are few and limited to *Ernstichthys* in the lower portions of western and central Amazon basin and drainages of the Brazilian Shield (e.g., Madeira and Tocantins; Ohara and Zuanon, 2013; and Jarduli et al., 2014), and the entire distribution of *Micromyzon akamai* (i.e., lowland Amazon River and lower portions of large tributaries; Friel and Lundberg, 1996; Ohara and Zuanon, 2013).

Most hoplomyzontin species inhabit deep channels of medium to large rivers (Stewart, 1985; Friel and Lundberg, 1996; Ohara and Zuanon, 2013). This habitat is relatively poorly sampled and, additionally, their small size may allow their escape from trawling equipment with larger mesh sizes. This may partly explain the relative paucity of specimens in museum collections. In rare cases, large collections of hoplomyzontins and another river channel aspredinid, *Xylophius*, have been made in dewatered riverbeds during dam construction (Taphorn and Marrero, 1990; Carvalho et al., in press a).

The specimens described here as a new species were collected during the 1978–1979 joint Venezuelan/USA Orinoco Delta Expeditions. The specimens were collected with bottom trawls from the R/V Eastward near Ciudad Guayana, Venezuela. The new species is known from just two specimens no larger than 15.6 mm SL. Given the constraint of sample size we used a non-invasive imaging technique, High-Resolution X-ray Computed Tomography (HRXCT or CT scan) to visualize and study their osteology, that allows their inclusion in a phylogenetic investigation of Aspredinidae. The HRXCT technology has been increasingly used to obtain comparative osteological data from rare species in museum collections (Schaefer, 2003; Rodiles et al., 2005; Schaefer and Fernández, 2009; Parisi and Lundberg, 2009; Carvalho and Albert, 2011; Carvalho et

al., in press a), and recent technical improvements make this a powerful tool for studying very small specimens (Lundberg et al., 2014; Carvalho et al., in press b).

MATERIAL AND METHODS

Measurements were taken point to point with digital calipers under a stereomicroscope. Measurements extending beyond the head are expressed as percent of the standard length (SL); dimensions of subunits of the head are expressed as percent of the head length (HL). The measurements follow those proposed by Friel (1995) and Cardoso (2010), except for cleithral-process length, which was taken from the anterior margin of cleithrum on its lateral portion along a horizontal to the posterior tip of the posterior cleithral process.

The holotype (ANSP 198335) was scanned at the High-Resolution X-ray Computed Tomography Facility, The University of Texas, Austin. It was scanned from the tip of snout to about the level of the third anal-fin ray with a NSI system Feinfocus source using the following settings, high power, 150 kV, 0.17 mA, no filter, Perkin Elmer detector, 0.25 pF gain, 2 fps (499.893 ms integration time), no binning, no flip, source to object 133.811 mm, source to detector 1316.553 mm, continuous CT scan, no frames averaged, 0 skip frames, 3000 projections, 6 gain calibrations, 0.762 mm calibration phantom, data range [-50, 500] (grayscale range adjusted from NSI defaults). Voxel size = 0.00948 mm. Total slices = 1308.

Visualizations and sectioning of the CT models were produced using the 16 bit TIFF files in VGStudio Max® V1.2.1, at the Ichthyology Department of the Academy of Natural Sciences, Philadelphia. Although the renderings appear similar to photographs, they represent the density differences of the biological materials as reflected in their X-ray opacity. Figures were prepared using still frames captured from digital animations of HRXCT and final preparation for publication was done using Adobe Photoshop® CS. The shadowing option in VGStudio was used to help visualize objects in 3D, and produced different effects in these images due to shape differences. Cut through videos along the axial, sagittal and frontal planes and raw images (8bit jpg) of X-ray slices were uploaded to Morphobank (www.morphobank.org), project number 2521.

Two dimensional digital radiographs of entire specimens ANSP 198335 and ANSP 200093 (paratype) were captured with a Kevex MicroFocus X-Ray Source and Varian PaxScan image receptor, and these were used to describe posterior body regions. Vertebral counts include all preural vertebrae, including the five vertebrae modified into the Weberian Apparatus, plus the PU1+U1 in the caudal

skeleton counted as a single vertebra. Specimens used for comparison were cleared and stained (cs) using the method described by Taylor and Van Dyke (1985). Photos were taken in a photo-tank following the techniques described by Sabaj Pérez (2009) with a Nikon D90 digital SLR.

Osteological descriptions focused on aspects and characters used in previous phylogenetic studies of the family Aspredinidae (Friel, 1994; de Pinna, 1996; Cardoso, 2008). Anatomical terminology generally follows the Teleost Anatomical Ontology (TAO; Dahdul et al., 2010) an integral part of the Uberon Ontology covering anatomical structures in animals (Mungall et al., 2012; <http://uberun.github.io/>). The dorsal and ventral vertebral processes are, respectively, dorsolateral and ventrolateral distally-flattened struts off the neural and hemal arches that form the dorsal and ventral body armor on the body surface (Taphorn & Marrero, 1990; fig. 4a; Friel and Lundberg, 1996). Institutional abbreviations follow Sabaj (2016).

***Micromyzon* Friel and Lundberg, 1996**

Type species.—*Micromyzon akamai* Friel and Lundberg, 1996: 642 by original designation.

Diagnosis.—Due to a more extensive review of material and the inclusion of an additional species into the formerly monotypic *Micromyzon*, it is necessary to amend the diagnostic characters of the genus. Therefore, the new composition of *Micromyzon* containing its type species and the herein newly described *Micromyzon* is diagnosed by the following apomorphic features: eyes absent (Figs. 1 and 2) vs. present; lateral margin of frontal straight, not forming an orbital concavity (Fig. 3A) vs. lateral margin of frontal concave, forming an orbital concavity; posterior cranial fontanel reduced by extended anterior ossification of parietal-supraoccipital (Fig. 3A, completely occluded by both parietal-supraoccipital and frontals in *M. akamai*) vs. posterior cranial fontanel extending posteriorly along the dorsal midline into parietal-supraoccipital; premaxilla absent or extremely reduced (Figs. 3 and 4) vs. premaxilla well developed; limb of autopalatine posterior to lateral ethmoid articulation about one fourth the length of anterior limb (Fig. 3) vs. limb of autopalatine posterior to lateral ethmoid articulation about one third or more the length of anterior limb; rows of large tubercles absent along posterior lateral line vs. conspicuous tubercles present on lateral line plates, anterior to lateral line pores; pigmentation reduced or absent, typical banding pattern of other hoplomyzontins of contrasting dark and clear areas on body subdued (Figs. 1 and 2) vs. pigmentation present, forming contrasting dark bands on dorsum and lateral portion of body.

Micromyzon orinoco* new species

Figures 1 and 2, Table 1

Undescribed *Hoplomyzon*.—Lundberg and Rapp Py-Daniel, 1994:387 [mentioned as undescribed].

Anophthalmic hoplomyzontine.—Friel and Lundberg, 1996:646 [mentioned as undescribed].

Holotype.—ANSP 198335, 15.6 mm SL, Venezuela, Anzoátegui, Río Orinoco, deep channel upstream of Los Barrancos, ca. 183 nautical miles from sea buoy in Boca Grande navigation channel, 08°21'N 062°43'W, J. N. Baskin, J. G. Lundberg and others, 14 Feb 1978.

Paratype.—ANSP 200093, 14.8 mm SL, Venezuela, Anzoátegui, Río Orinoco, north-side of Isla Fajardo, opposite to Palua, 182 nautical miles from sea buoy, 08°22'N 62°42'W, J. N. Baskin, H. López and others, 6 Nov 1979.

Diagnosis.—The new species differs from *Micromyzon akamai* by having the anterior margin of the mesethmoid straight (Fig. 3A, vs. anterior margin with a medial notch); posterior cranial fontanel open (Fig. 3A, vs. posterior cranial fontanel closed); first pectoral-fin radial ossified (vs. first pectoral-fin radial completely cartilaginous); a single tubular infraorbital bone (Fig. 3A, vs. three tubular infraorbital bones); infraorbital sensory canal entering neurocranium via frontal (Fig. 3A, vs. infraorbital sensory canal entering neurocranium via sphenotic); occluded foramen for the *abductor superficialis* muscle in the coracoid (Fig. 9, vs. open foramen for the *abductor superficialis* in the coracoid); higher vertebral count: 33 (vs. 28–32 vertebrae); higher anal-fin ray count: 10 or 11 (vs. 7–9 anal-fin rays). Additionally, *Micromyzon orinoco* differs from *M. akamai* by the following morphometric features: longer pectoral-fin spine, 26.9–28.4% SL (vs. 12.0–20.0% SL); longer anal-fin base, 22.3–22.4% SL (vs. 16.1–22.2% SL); longer caudal fin, 30.1–31.1% SL (18.2–27.2% SL); and shorter caudal peduncle, 23–25% SL (vs. 25.2–32.2% SL).

Description.—Morphometric data summarized in Table 1. Head and body depressed (Fig. 1). Dorsal profile rising from snout tip to dorsal-fin origin with humps at posterior margin of infraorbital 1 and above orbit, and pronounced midline humps at posterior portion of parietal-supraoccipital, posterior end of dorsal blade of Weberian complex vertebrae and middle nuchal plate, then descending gradually to end of caudal peduncle; ventral profile straight to slightly convex from mouth

*LSID urn:lsid:zoobank.org:act:89657AD6-1D1C-40BA-B4DB-3A2E89611F45

to anus, ascending from that point to end of anal fin, almost straight from that point to posterior end of caudal peduncle. Infraorbital 1 elevated over main margin of head surface, somewhat hook-shaped at its posterior margin. Rostrum rounded to slightly pointed in dorsal view, lacking medial notch (Figs. 1 and 2). Head relatively narrow with pointed snout, body widest at pectoral-fin insertion. Caudal peduncle long and slender, somewhat squared in cross section.

Eyes absent. Anterior nares located dorsally closer to snout tip than to posterior nares, enclosed by fleshy tube; anterior margin of tube with small flap-like papilla. Posterior nares lacking fleshy tube, but having two small dermal flaps on its anterior margin, posterior nares aligned and medially offset relative to posterior portion of infraorbital 1. Rostrum overhanging ventrally displaced mouth; gape small, arrowhead shaped in ventral view. Papillae absent on upper and lower lips.



Fig. 1. *Micromyzon orinoco*, holotype, ANSP 198335, 15.6 mm SL, Río Orinoco, deep channel upstream of Los Barrancos, ca. 183 nautical miles from sea buoy in Boca Grande navigation channel, Anzoátegui, Venezuela, 08°21'N 062°43'W. Dorsal, left side lateral and ventral views.



Fig. 2. *Micromyzon orinoco*, paratype, ANSP 198335, 14.8. mm SL, Río Orinoco, north-side of Isla Fajardo, opposite Palua, 182 nautical miles from sea bouy, Anzoátegui, Venezuela, 08°22'N 62°42'W. Dorsal and ventral views.

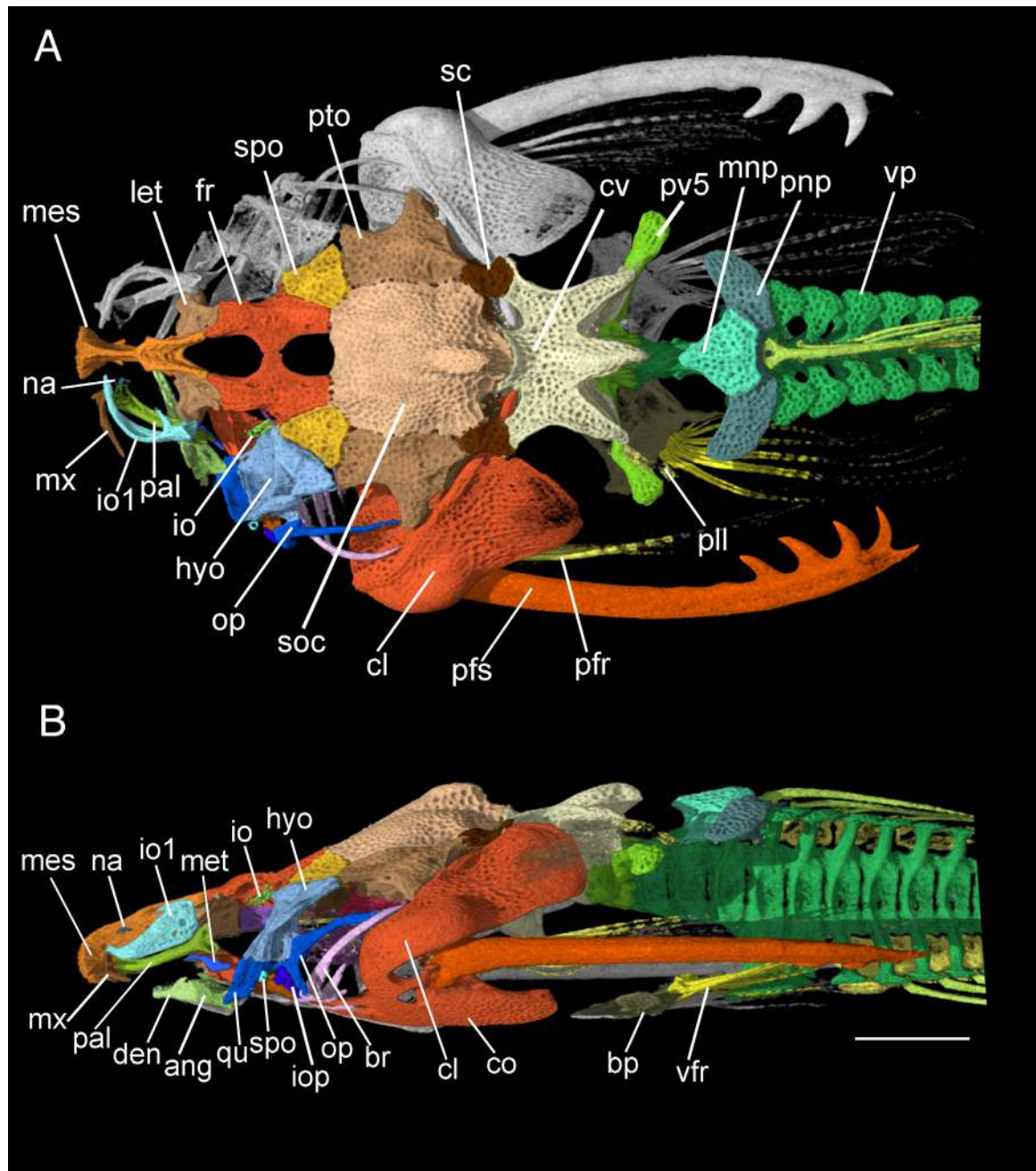


Fig. 3. HRXCT model of skull and anterior body of *Micromyzon orinoco*, holotype, ANSP 198335, 15.6 mm SL. A. Dorsal view. B. Lateral view of left side. ang: anguloarticular; bp: basipterygium; br: branchiostegal rays; cl: cleithrum; co: coracoid; cv: Weberian complex vertebra; den: dentary; fr: frontal; hyo: hyomandibula; io: last infraorbital tubule; io1: infraorbital 1; iop: interopercle; let: lateral ethmoid; mes: mesethmoid; met: metapterygoid; mnp: middle nuchal plate; mx: maxilla; na: nasal; op: opercle; pal: autopalatine; pfr: pectoral-fin rays; pfs: pectoral-fin spine; pll: posterior lateral line; pnp: posterior nuchal plate; pto: pterotic; pv5: parapophysis of fifth vertebra; qu: quadrate; sbo: subpreopercle; sc: posttemporo-supracleithrum; soc: parietal-supraoccipital; spo: sphenotic; vfr: pelvic-fin rays; vp: dorsal vertebral process. Scale bar = 1 mm.

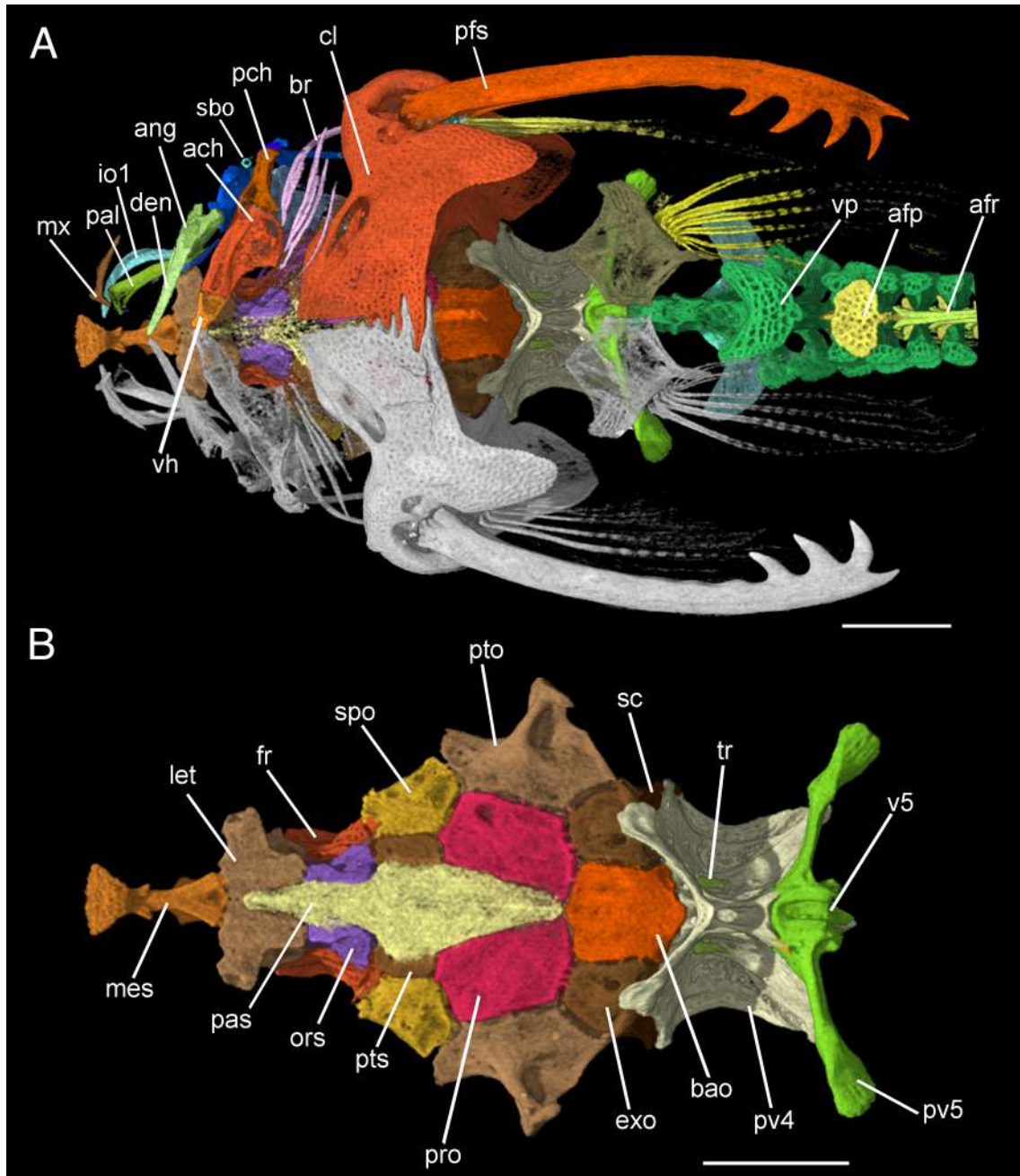


Fig. 4. HRXCT model of skull and anterior body of *Micromyzon orinoco*, holotype, ANSP 198335, 15.6 mm SL. A. Ventral view of skull and anterior body. B. Ventral view of neurocranium and first vertebrae. ang: anguloarticular; ach: anterior ceratohyal; afp: anal-fin pterygiophore; afr: anal-fin ray; bao: basioccipital; br: branchiostegal rays; cl: cleithrum; den: dentary; exo: exoccipital; fr: frontal; let: lateral ethmoid; mes: mesethmoid; mx: maxilla; ors: orbitosphenoid; pal: autopalatine; pas: parasphenoid; pch: posterior ceratohyal; pfs: pectoral-fin spine; pro: prootic; pts: pterosphenoid; pto: pterotic; pv4: parapophyses of compound centrum; pv5: parapophyses of fifth vertebra; sp: subpreopercle; sc: posttemporo-supracleithrum; spo: sphenotic; tr: tripus; vh: ventral hypophyal; v5: vertebra 5; vp: ventral process of vertebra. Scale bar = 1 mm.

Three main pairs of barbels, all simple. Maxillary barbel short, almost reaching to anterior margin of cleithrum, with medial membrane adnate to snout and head; membrane contacting head almost reaching to straight vertical line with posterior pair of mental barbel. Mental barbels short, posterior pair laterally displaced, separated from counterpart about three times distance of separation of anterior pair. Posterior mental barbel about three times length of anterior mental barbel. Three pairs of rictal barbels at axillary portion of maxillary barbel membrane between barbel and head. Two pairs of rictal barbels small, smaller pair displaced near lateral margin of mouth and larger, almost same size of anterior mental barbel, and displaced at ventral and proximal portion of maxillary barbel. Additional series of small barbel-like papillae scattered over ventral portion of head. Opercular opening small, transversely oriented relative to main body axis at ventral portion of head, and concealed by rounded membranous flap. Opercular openings separated by distance of about three times length of their apertures. Skin of body smooth, without rounded and unicuspid unculiferous tubercles. Small, oblique, slit-like pore at pectoral-fin axilla ventral to posterior cleithral process.

External surface of skull roof bones with pitted texture, and somewhat interdigitating sutures between bones. Mesethmoid long and deep; its middle portion strongly constricted in dorsal view and slightly elevated in lateral view. Anterior margin of mesethmoid convex and smooth, medial notch absent; weakly projecting cornua laterally (Figs. 3 and 4). Ventral portion of mesethmoid with laterally displaced barb-like process. Posterior contact of mesethmoid with frontal flat, dorsally projecting processes absent. Lateral ethmoid extended posterodorsally, but not contributing to dorsal surface of neurocranium. Antorbital process of lateral ethmoid extended laterally, articulating with mesial surface of autopalatine. Frontal compact (length similar to its width), slightly constricted at middle. Frontal contacting sphenotic posterolaterally and parietal-supraoccipital posteriorly via extended arms. Anterior cranial fontanel ovoid, long (length about twice its width), its anterior third surrounded by mesethmoid, remainder by frontals and epiphyseal bridge. Posterior cranial fontanel anteriorly rounded and short, flanked laterally by frontals and its posterior margin almost transversely straight and limited by parietal-supraoccipital (Fig. 3A). Epiphyseal bar with small medial suture (suture length narrower than cranial fontanels). Parietal-supraoccipital compact, its greatest length about same as greatest width, somewhat round in dorsal view. Anterior margin of parietal-supraoccipital straight, without anteriorly expanded lateral arm, contacting frontal medially, sphenotic anterolaterally, pterotic laterally and posttemporo-supracleithrum posterolaterally. Posterior

process of parietal-supraoccipital truncated and rounded, extensively contacting Weberian complex vertebrae posteriorly. Sphenotic somewhat triangular in dorsal view, its posterior margin contacting pterotic laterally; and extensively articulating with hyomandibula anterolaterally. Pterotic somewhat expanded anterolaterally, contacting sphenotic and hyomandibula; forming strongly concave margin with greatly expanded lateral shelf. Pterotic wing laterally expanded shelf with somewhat pointed margin. Supratemporal fossa absent, slight concavity at its typical position between pterotic and parietal-supraoccipital. Extrascapula absent. Posttemporo-supracleithrum plate-like with pitted surface, contributing to dorsal surface

Table 1. Morphometric data of holotype and paratype of *Micromyzon orinoco*.

	H	P	Mean
Standard length (mm)	15.6	14.8	
	Percent of Standard Length		
Head length	26.3	27.7	27.0
Prepectoral length	26.9	27.0	27.0
Cleithral width	29.5	33.1	31.3
Maximum head depth	14.7	14.9	14.8
Pectoral-spine length	26.9	28.4	27.7
Distance between coracoid processes	17.3	18.9	18.1
Coracoid process length	5.76	7.43	6.6
Distance between cleithral processes	22.4	25.0	23.7
Cleithral process length	14.7	12.1	13.5
Predorsal length	41.7	43.9	42.8
Depth at dorsal-spine insertion	14.7	14.9	14.8
Dorsal-spine length	13.5	13.5	13.5
Prepelvic length	35.9	38.5	37.2
Length of 1 st pelvic-fin ray	14.1	14.9	14.5
Preanal length	49.3	51.3	50.4
Anal-fin base length	22.4	22.3	22.4
Caudal-peduncle length	25.0	23.0	24.0
Caudal-peduncle depth	4.5	4.0	4.3
Caudal-fin length	30.1	31.1	30.6
	Percent of Head Length		
Maxillary-barbel length	24.4	21.9	23.2
Distance between anterior nares	56.1	51.2	53.7
Distance between posterior nares	21.9	19.5	20.7
Mouth width	26.8	26.8	26.8

of skull; contacting pterotic and parietal-supraoccipital anteriorly and Weberian complex centrum posteriorly. Dorsal foramen bounded by posttemporo-supracleithrum laterally, Weberian complex centrum posteriorly and parietal-supraoccipital anteriorly (Fig. 3A). Posttemporo-supracleithrum strongly sutured with surrounding bones and expanded laterally at contact with parapophysis of Weberian complex vertebra.

Vomer absent. Parasphenoid relatively short, its anterior margin not surpassing anterior margin of lateral ethmoid; its posterior margin just reaching anterior limit of basioccipital; broadest at about its middle portion (Fig. 4B). Orbitosphenoid and pterosphenoid lateroventrally displaced; former larger than latter. Prootic somewhat square in shape (ventral view), Trigemino-facial foramen not clearly observed. Basioccipital square in shape (ventral view), contacting prootic anteriorly and extensively contacting basioccipital posteriorly. Epiotic apparently absent or fused with exoccipital, not contributing to dorsal surface of neurocranium, exoccipital extensively contacting basioccipital medially and slightly contacting Weberian complex vertebra posteriorly.

Premaxilla absent. Maxilla long and slender, distally bifurcate for about two-thirds its length with ventrolateral arm longer than dorsomedial one. Anterior portion of maxilla with two rounded articular processes, contacting anterior surface of autopalatine. Dentary slender, not contacting counterpart medially; teeth villiform, extending to about midlength of dentary (Fig. 5). Anguloarticular with dorsally expanded process, as typical posterior portion of coronoid process. Anguloarticular strongly fused with retroarticular (articular-angular-retroarticular), both forming socket for joint with quadrate. Coronomeckelian bone absent.

Hyomandibula with slightly protruding anterodorsal process contacting ventral face of frontal-sphenotic joint. Hyomandibula with concave anteroventral face, extensively contacting quadrate by interdigitating suture; fused with preopercle laterally. Hyomandibula with elongate posteroventrally directed opercular condyle on its posterior margin. Preopercle strongly fused with lateral margin of hyomandibula. Preopercle with well-developed, laterally directed expansion. Suprapreopercle absent. Quadrate subtriangular, not contacting ventral margin of metapterygoid dorsally (except perhaps by pterygo-quadrate cartilage). Subpreopercle ossified as tubular canal positioned ventrally to quadrate (Figs. 3 and 4A). Entopterygoid absent, (perhaps fused with anterior portion of metapterygoid). Metapterygoid elongate, constricted at its midlength. Anterior margin of metapterygoid reaching antorbital process of lateral ethmoid. Autopalatine elongate, contacting lateral ethmoid at about its third fourth of length,

posterior end slightly bifurcate and laterally compressed. Opercle boomerang shaped with dorsal wing about three times as long as ventral wing. Interopercle present, wedge shaped with posterodorsal margin firmly attached to anterior margin of ventral wing of opercle (Fig. 5).

Dorsal hypohyal absent (Fig. 6). Ventral hypohyal somewhat triangular in dorsal view, contacting anterior ceratohyal laterally by interdigitated suture. Anterior ceratohyal broad, its anterior margin somewhat straight without expanded blade. Posterolateral margin of anterior ceratohyal greatly expanded. Larger than its interdigitating sutural joint with posterior ceratohyal, contacting posterior ceratohyal via (Fig. 6B). Posterior ceratohyal somewhat triangular in shape, tapering laterally. Interhyal absent. Four branchiostegal rays; outermost (fourth) with anterior half expanded ventrally as posteriorly elongate blade, posterior portion greatly curved inwards; third branchiostegal expanded posteriorly distal to its midpoint; remaining branchiostegals 3 and 4 shorter and slender. Branchial arches weakly ossified (or decalcified). Urohyal, basibranchials and hypobranchials not ossified. Five ceratobranchials bearing short gill rakers; acicular teeth on dorsal margin of fifth ceratobranchial. Four epibranchials, first and second

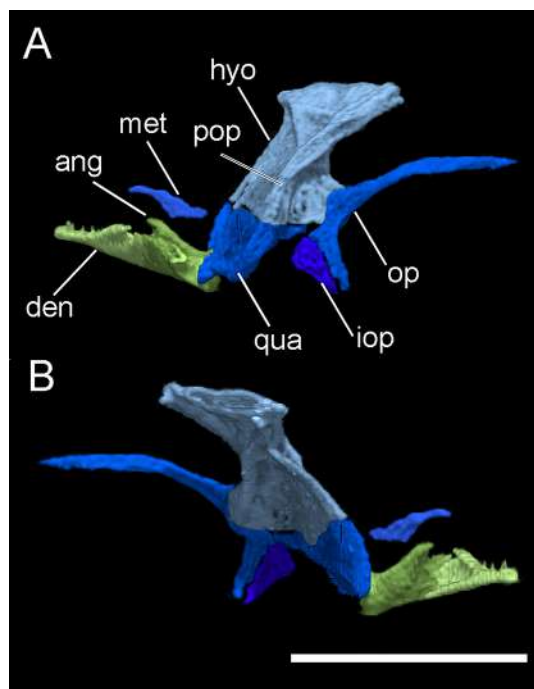


Fig. 5. HRXCT model of left side suspensorium and lower jaw of *Micromyzon orinoco*, holotype, ANSP 198335, 15.6 mm SL. A. Lateral view. B. Medial view. ang: anguloarticular; den: dentary; hyo: hyomandibula; iop: interopercle; met: metapterygoid; op: opercle; qua: quadrate. Scale bar = 1 mm.

slender and third and fourth broader; third bearing uncinat process. Dorsal tooth plate bearing elongate acicular teeth, bony pharyngobranchials not observed.

Nasal small and tubular, positioned lateral to constricted portion of mesethmoid (Fig. 3A). Infraorbital 1 slender, with anteriorly elongated arm curved medially around the olfactory organ fossa plus shorter, medially directed pointed process. Infraorbital canal entering medial margin of infraorbital 1 just posterior to medially directed process and exiting at posterior portion on lateral surface. Remaining infraorbital bone reduced to small, disjointed and tubular ossicle anterior to entrance on frontal. Preoperculo-mandibular canal incomplete, anterior portion absent, remaining represented by single short tubular ossification (subpreopercle) anterior to lower foramen in preopercle. Posterior portion of preoperculo-mandibular canal associated to posterodorsal portion of hyomandibula and entering pterotic dorsally. Postotic canal exiting at posterior portion of pterotic and entering anterior portion of posttemporo-supracleithrum. Pterotic branch exiting laterally at posterior portion of pterotic and first branch of main lateral line exiting posttemporo-supracleithrum posterolaterally. Body lateral line sensory canal embedded within parapophyses of Weberian complex vertebrae, exiting posterolateral portion of that bone and entering posterior lateral-line canal tubules (Fig. 3A). Posterior lateral line complete, reaching hypural region posteriorly. Posterior lateral line straight on midlateral portion of body; not associated with dorsally and ventrally expanded plate-like structures (lateral plates) on anterior portion of body. Weakly ossified lateral plates, associated with lateral line ossified tubules on posterior portion of body, posterior to vertical through middle of anal fin.

Neural arch and spine of Weberian complex vertebra reaching to dorsal surface of body, its dorsal surface strongly concave anteriorly and elevated in hump posteriorly (Figs. 3B, 7). Parapophysis of Weberian complex vertebra moderately short (length about equal to width), its posterior margin extensively contacting parapophysis of fifth vertebra. Ventral portion of Weberian complex vertebra with ventral process forming arch over aortic canal and additional laterally directed arms; these arms with expanded thin bony vertical blades that surround gas bladder anteriorly (Figs. 4 and 7). Parapophysis of fifth vertebra long, extending beyond lateral limits of parapophysis of fourth vertebra and reaching to body wall. Parapophysis of fifth vertebra directed posteriorly with distal margin slightly expanded and hollow. Anterior nuchal plate absent. Middle nuchal plate smaller than posterior nuchal plate, somewhat diamond-shaped in dorsal view (Fig. 8A) and posterolaterally extensively contacting posterior nuchal plate (Fig. 8A, B). Middle nuchal plate distant from dorsal keel of Weberian

complex vertebrae. First dorsal-fin (middle nuchal plate) pterygiophore ventrally contacting sixth, seventh and eighth vertebrae. Posterior nuchal plate expanded anterolaterally, wing-shaped with rounded lateral tip. Second dorsal-fin (posterior nuchal plate) pterygiophore ventrally contacting eighth vertebra and posteriorly overlapping dorsal process of ninth vertebra. Vertebrae 9 and 10 to last or penultimate vertebrae bearing dorso- and ventrolateral projecting processes that serially overlap (Fig. 8). Ventrally directed processes of vertebra 9 and 10 expanded laterally, exposed ventral surface ventrally concave anteriorly and rounded posteriorly. Ventrally directed process of vertebrae 10 and 11 not extending ventrally to body surface. Dorsally and ventrally directed vertebral processes bifid under dorsal and anal fin; fused medially posterior to last vertebrae associated with pterygiophores of those fins (Fig. 8). Two foramina for hemal canal; on anteroventral portions of vertebrae 6 and 9. Hemal and neural spines short except for hemal spines associated with last two vertebrae; hemal spines associated with anal-fin pterygiophores slightly bifid. Consecutive

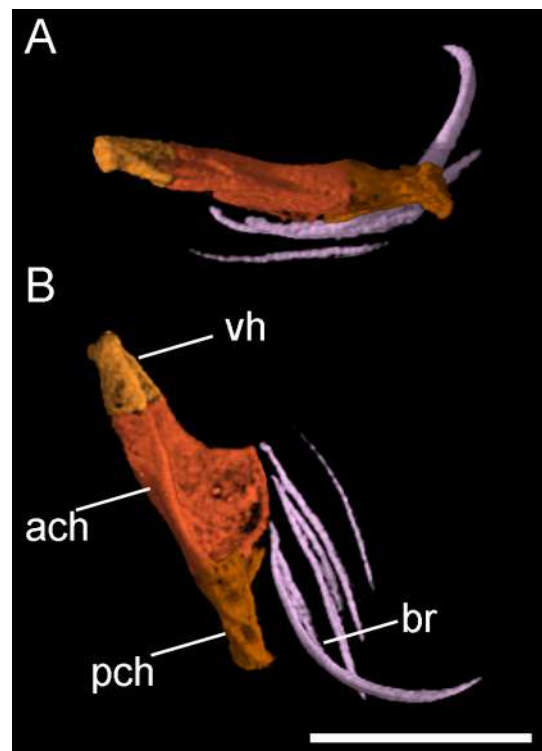


Fig. 6. HRXCT model of hyoid arch of *Micromyzon orinoco*, holotype, ANSP 198335, 15.6 mm SL A. Left side in lateral view. B. dorsal view (anterior towards left). ach: anterior ceratohyal; br: branchiostegal rays; pch: posterior ceratohyal; vh ventral hypohyal. Scale bar = 1 mm.

vertebrae articulated by interdigitating joints between serially adjacent neural and hemal arches. Ribs absent. Hypurals fused; ventral lobe of caudal skeleton slightly longer than dorsal lobe, with greatly pronounced diastema between upper and lower hypural plates. Hypurapophysis elongate and greatly expanded laterally.

Dorsal-fin i,4. Dorsal-fin spinelet absent. First dorsal-fin ray simple (not pungent or rigid), slender but thicker than following branched dorsal-fin rays. Last dorsal-fin

ray likely adnate to dorsum by currently torn membrane. Adipose fin absent.

Anal fin 10 or 11 total rays (4 and 5 anterior rays unbranched); last ray not adnate. Caudal fin with nine principal rays, five in dorsal and four in ventral lobe; distal margin obliquely truncate with lower lobe slightly longer than upper. Outermost principal caudal-fin ray unbranched and expanded proximally. Procurent caudal-fin rays small; difficult to visualize in radiographs.

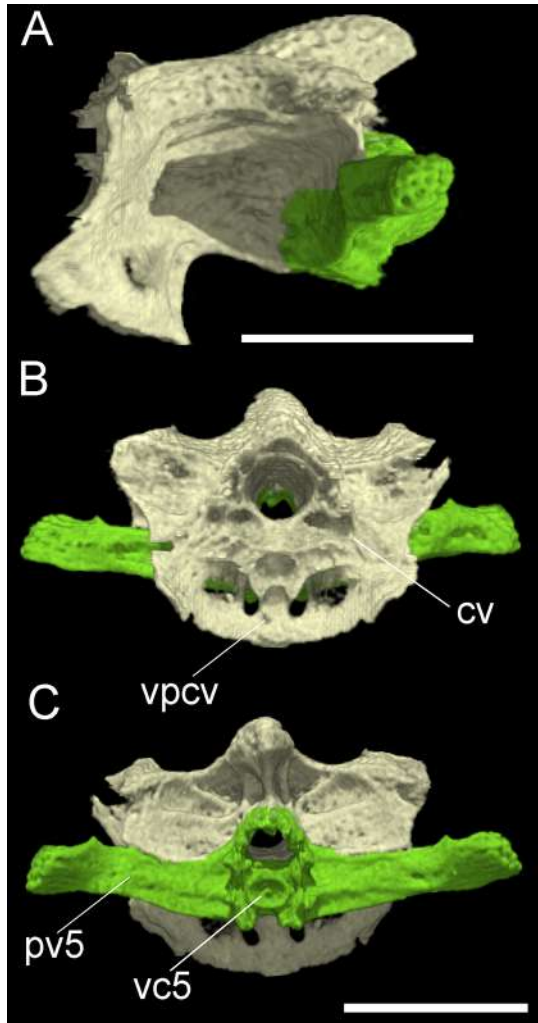


Fig. 7. HRXCT model of Weberian complex vertebra and fifth vertebrae of *Micromyzon orinoco*, holotype, ANSP 198335, 15.6 mm SL. A. Lateral (anterior towards left). B. Front view. C. Back view. cv: Weberian complex vertebra; pv5: parapophysis of fifth vertebra; vc5: vertebral centrum of fifth vertebra; vpcv: ventral process of Weberian complex vertebra. Scale bar = 1 mm.

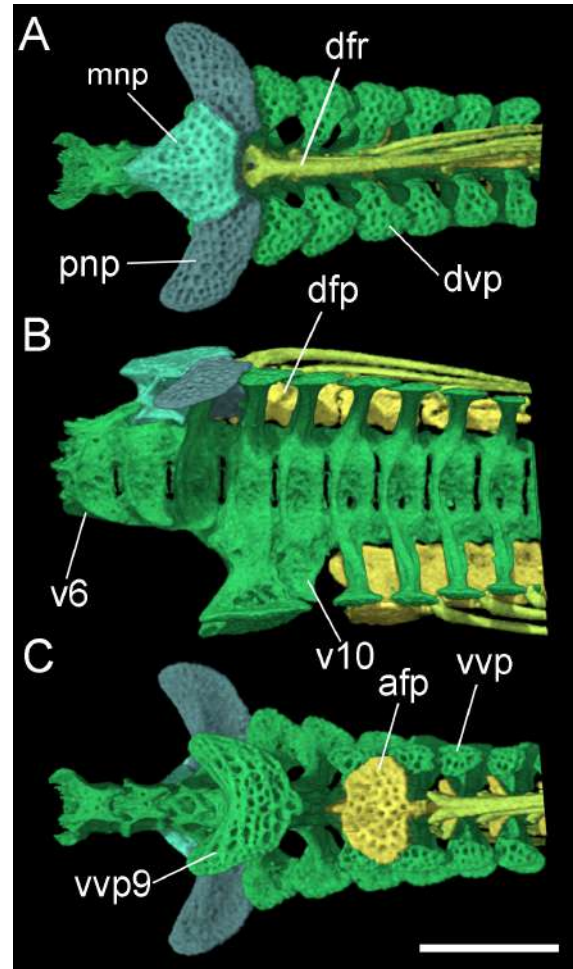


Fig. 8. HRXCT model of vertebrae and associated dorsal and anal fin structures of *Micromyzon orinoco*, holotype, ANSP 198335, 15.6 mm SL. A. Dorsal view; B. lateral view and C. ventral view (anterior portion towards left). afp: anal-fin pterygiophore; dfp: dorsal-fin pterygiophore; dfr: dorsal-fin rays; dvp: dorsal vertebral process; mnp: middle nuchal plate; pnp: posterior nuchal plate; v6: sixth vertebra; v10: tenth vertebra; vvp: ventral vertebral process of vertebra nine; vvp9: ventral vertebral process of vertebra nine. Scale bar = 1 mm.

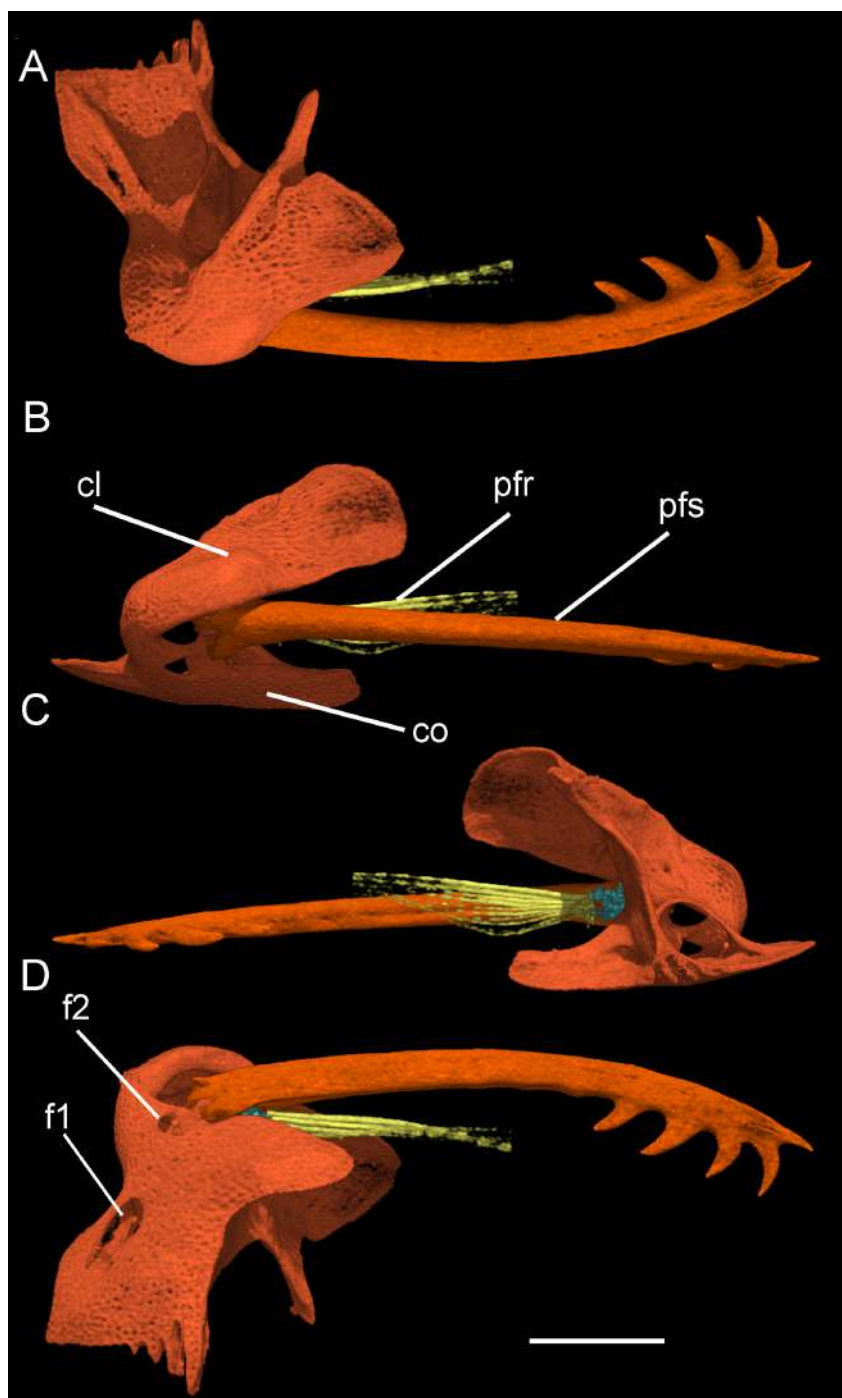


Fig. 9. HRXCT model of left pectoral skeleton of *Micromyzon orinoco*, holotype, ANSP 198335, 15.6 mm SL. A. Dorsal view (anterior towards left). B. Lateral view (anterior towards left). C. Medial view (anterior towards right). D. Ventral view (anterior towards left). cl: cleithrum; co: coracoid; f1: Cleithral *arrector dorsalis* muscle foramen; f2: Cleithral *arrector superficialis* muscle foramen; pfr: pectoral-fin rays; pfs: pectoral-fin spine. Scale bars = 1 mm.

Pectoral fin I,5. First ray spine-like, long and distally pointed; following rays branched. Pectoral-fin spine slightly curved. Anterior margin of pectoral-fin spine smooth; posterior margin with 3 or 4 strong posterior dentations restricted to distal portion and diminishing in size proximally (Fig. 9). Dorsal portion of cleithrum with two processes: dorsal process long and narrow with lateral cleft; process articulating with ventral portions of supracleithrum and parapophysis of Weberian complex centrum; posterior dorsal process variable somewhat broad and rounded in holotype (Fig. 9A), but considerably pointed in paratype (examined by X-ray). Cleithrum and coracoid partially fused, sutures almost indistinguishable. Anteromedial margin of cleithrum straight; deeply concave laterally. Cleithrum counterparts with simple abutting joint, coracoid with strongly and extensive interdigitating ventromedial symphysis (Figs. 4A and 9A, D). Cleithrum bearing two small foramina on its ventral blade: anteromedial foramen positioned parallel to anterior concavity of cleithrum (Fig. 9: f1) and lateral one smaller, positioned near articulation with pectoral-fin spine (Fig. 9: f2). Lateral foramen in coracoid absent (Fig. 9B, C). Coracoid bearing short and posteriorly directed process with rounded and pointed posterior margin (Figs. 4A and 9C).

Pelvic fin i,5; second ray longest, surpassing anal-fin origin. Anterolateral process of basipterygium weakly developed, anteromesial process somewhat triangular and pointed anteriorly (Fig. 10A). Basipterygium with smooth anterior and posterior margins; with posteriorly elongate pointed process. Basipterygium with dorsal process in its central position.

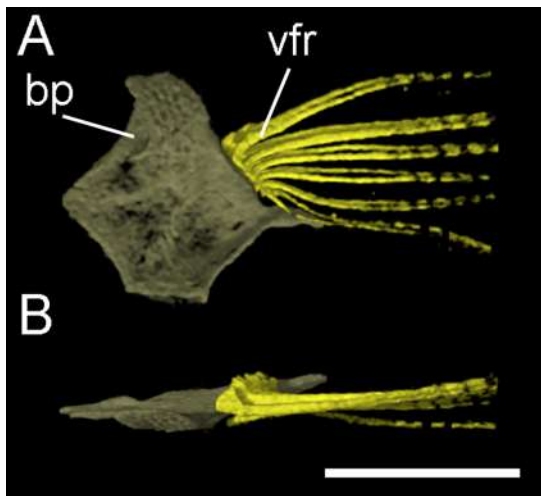


Fig. 10. HRXCT model of pelvic girdle of *Micromyzon orinoco*, holotype, ANSP 198335, 15.6 mm SL. A. Dorsal view; B. lateral view. bp: basipterygium; vfr: pelvic-fin rays. Scale bar = 1 mm.

Coloration.—Pigmentation greatly reduced or absent in alcohol preserved specimens on body and fins (Figs. 1 and 2). A photo taken of ANSP 200093 just after fixation shows a few chomatophores along middorsal region of body posterior to dorsal fin.

Distribution and habitat.—The new species is known from two localities in the lower Orinoco River in Venezuela near the town of Ciudad Guayana (Fig. 11). This species was collected with trawl nets in the main channel of the Orinoco River, at depths of 10 and 18 meters on a sandy and muddy bottom. Plastic fly screen of small mesh size lined the posterior end of the trawl net, and trawling was done downstream for about 25 minutes. The specimens were collected with a variety of gymnotiform species including *Gymnorhamphichthys hypostomus*, *Rhamphichthys apurensis*, *Steatogenys elegans*, *Sternachorhynchus* sp., *Sternarchogiton nattereri*, *Sternarchorhamphus muelleri*, *Eigenmannia macrops*, *Adontosternarchus sachsii*, *A. devenanzii*, *Sternarchella orinoco*, *S. orthos*, and *Rhabdolichops troscheli*, and siluriforms including *Megalonema orixanthum*, *Pinirampus pirinampu*, *Cetopsis coecutiens*, *Pterodoras rivasi* and *Leptodoras rogersae*.

Etymology.—The specific epithet, *orinoco*, is in reference to the known distribution of the new species, Río Orinoco. A noun in apposition.

DISCUSSION

The new species shares five of the eight characters proposed by Friel and Lundberg (1996) as diagnostic for *Micromyzon*. Considering the putative relationships of this genus within the Hoplomyzontini as sister to a group formed by *Dupouyichthys* and *Ernstichthys* (Friel and Lundberg, 1996), these features are interpreted as synapomorphies for the genus. Such features are: eyes absent (Figs. 1 and 2, 12A); premaxillae extremely reduced or absent (Fig. 4); limb of autopalatine posterior to lateral ethmoid articulation much shorter than anterior limb (about one fourth of anterior limb; Fig. 3A, 12B); absence of rows of large tubercles along lateral line and posterior portion of body; and reduced pigmentation without the typical banding pattern of other hoplomyzontins (Figs. 1 and 2). Another condition of *Micromyzon akamai* noted by Friel and Lundberg (1996) is the reduced anterior cranial fontanel and occluded posterior cranial fontanel. Partial occlusion of the fontanels is also observed in *M. orinoco*. In the new species, the posterior cranial fontanel is reduced in size by increased growth of the anterior portion of the parietal-supraoccipital over the posterior

limits of the fontanel (Fig. 3A). Contrastingly, in *M. akamai* bone growth over the posterior fontanel is made by both the parietal-supraoccipital and the frontal bones (Fig. 12B; Friel and Lundberg, 1996: fig. 2). Therefore, the reduction of the posterior cranial fontanel by anterior growth of the parietal-supraoccipital can be considered a synapomorphy for *Micromyzon*, and this is not observed in other hoplomyzontins and all other aspredinids (except *Acanthobunocephalus nicoi*; Friel, 1995: fig. 2).

Another feature previously proposed to diagnose *Micromyzon* is the reduced or absent paired foramina bordered by the supracleithrum, parietal-supraoccipital and Weberian complex (Friel and Lundberg, 1996: fig. 2). Further investigation on Hoplomyzontini does not show conspicuous differences among taxa in the size of those foramina. This is likely intraspecifically variable within *M. akamai*, and therefore is not particularly useful for diagnosing *Micromyzon* (see for comparison CT reconstruction of *M. akamai* on Catfishbones Atlas (<http://catfishbone.ansp.org/Aspredinidae/Micromyzon/catscan.html>)).

Other features proposed as synapomorphies for *Micromyzon*, such as hypertrophied lateral-line ossicles forming an armor of overlapping crescent-shape plates with dorsal and ventral limbs tilted anteriorly (Friel and Lundberg, 1996: fig. 3); short, rounded posterior process of cleithrum; and very short posterior coracoid processes, not extending past anterior limit of basipterygia, are likely apomorphic for *Micromyzon akamai* (the last feature seen elsewhere within Hoplomyzontini, e.g. and undescribed species of *Hoplomyzon*).

Both species of *Micromyzon* are miniatures reaching only to 15 or 16 mm SL. Body size reduction also characterizes other hoplomyzontins, such as an undescribed species of *Hoplomyzon* (18.5 mm SL;

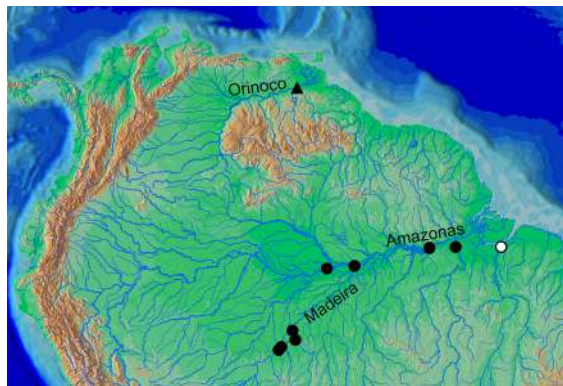


Fig. 11. Distributions of species of *Micromyzon* in the Amazon and Orinoco basins based on examined museum specimens. Triangle: *Micromyzon orinoco*. Circles: *Micromyzon akamai* (white filled circle represents type locality).

Carvalho et al., in press b) and *Hoplomyzon papillatus* (19.4 mm SL). Despite the fact that most miniature fishes display pedomorphic features indicated by reduced skeletons and fin-ray counts (Weitzman and Vari, 1988), hypermorphic characters are also known from other miniature catfishes such as scoloplacids (Schaefer et al., 1989) and the hoplomyzontins (Friel and Lundberg, 1996). Hypermorphic features such as the hypertrophied development of the parietal-supraoccipital and reduction of the posterior cranial fontanel are also observed in the miniature aspredinids *Acanthobunocephalus nicoi* (Friel, 1995) and *M. akamai* (Fig. 12; as already discussed by Friel and Lundberg, 1996). According to Friel and Lundberg (1996), the reduction of fontanels in *M. akamai* would strengthen the cranium and complement the well-developed body armor of that taxon. Both features are in line with the hypothesis of Taphorn and Marrero (1990) that strong body armor would prevent those fishes from being crushed by shifting substrate in rapid flowing waters. As discussed above, *M. orinoco* has also a relative reduction of the size of the posterior cranial fontanel, but extreme reduction of lateral plates contrasting with *M. akamai* and other hoplomyzontins, perhaps indicating that such features are decoupled. An additional feature that may indicate hypermorphosis is the overgrowth of laminar bone over the typical median empty area in the pectoral girdle bridge seen in other hoplomyzontins (Taphorn and Marrero, 1990: fig. 2; Carvalho et al., in press b). This character state may be a reversal of an apomorphic condition observed in other genera in the tribe and therefore an additional synapomorphy for *Micromyzon*.

Members of Hoplomyzontini are commonly found in the deep channels of large white water rivers, lightless environments that have relatively rapid flowing waters (Stewart et al., 2002). *Micromyzon* has apomorphic adaptations to this environment such as eye reduction and loss of pigmentation, characteristics that are noted for other fishes inhabiting this environment (Fig. 12A; Lundberg and Py-Daniel, 1994, Carvalho et al. in press a). Within the Aspredinidae, the independent reduction of pigmentation and loss of eyes occurred at least twice, being observed in *Micromyzon* and another species of *Xyliphius* from the main channel of the Amazon River in Peru (Carvalho et al., in press a). In both cases, eyeless and unpigmented species are closely related to taxa that inhabit similar environments in the Amazon, Orinoco and Paraná-Paraguay systems, indicating a less pronounced habitat shift. Other adaptations observed in fishes from these habitats include small size, flattened or elongated body, ventral mouth, and sensory specializations (Stewart et al., 2002); all of these observed to some degree in hoplomyzontins.

MATERIAL EXAMINED

In addition to the material listed in previous publications (Carvalho et al., 2015, in press a, b; and Friel and Carvalho, 2016), the following lots of *Micromyzon akamai* were examined: all from Brazil. ANSP 180358, 2, 14.2-15.4 mm SL, Amazonas, rio Solimões below rio Purus and upstream Manacapuru, 03°27'02"S 60°45'07"W. ANSP 180882, 6 (2 cs), 12.3-12.7 mm SL, Amazonas, rio Amazonas downstream Nova Oriente, 03°16'52"S 58°56'27"W. ANSP 182777, 1, not measured, Amazonas,

rio Amazonas above rio Madeira, 3 miles downstream Nova Oriente, 03°16'51"S 58°56'30"W. ANSP 195263, 2, 13.3-13.7 mm SL, Amazonas, rio Amazonas above rio Madeira, 3 miles downstream Nova Oriente, 03°16'51"S 58°56'30"W. ANSP 195264, 1, 14.1 mm SL, Pará, rio Amazonas below rio Tapajós, 10.2 km upstream from Monte Alegre, 02°05'28"S 54°00'22"W. ANSP 195265, 1, 14.5 mm SL, rio Acaraí, 5 km upstream from confluence with rio Xingu, 02°02'16"S 52°16'56"W. CUMV 82545, 1, 14.1 mm SL, Pará, rio Amazonas south bank of river about 155 km downstream from mouth of

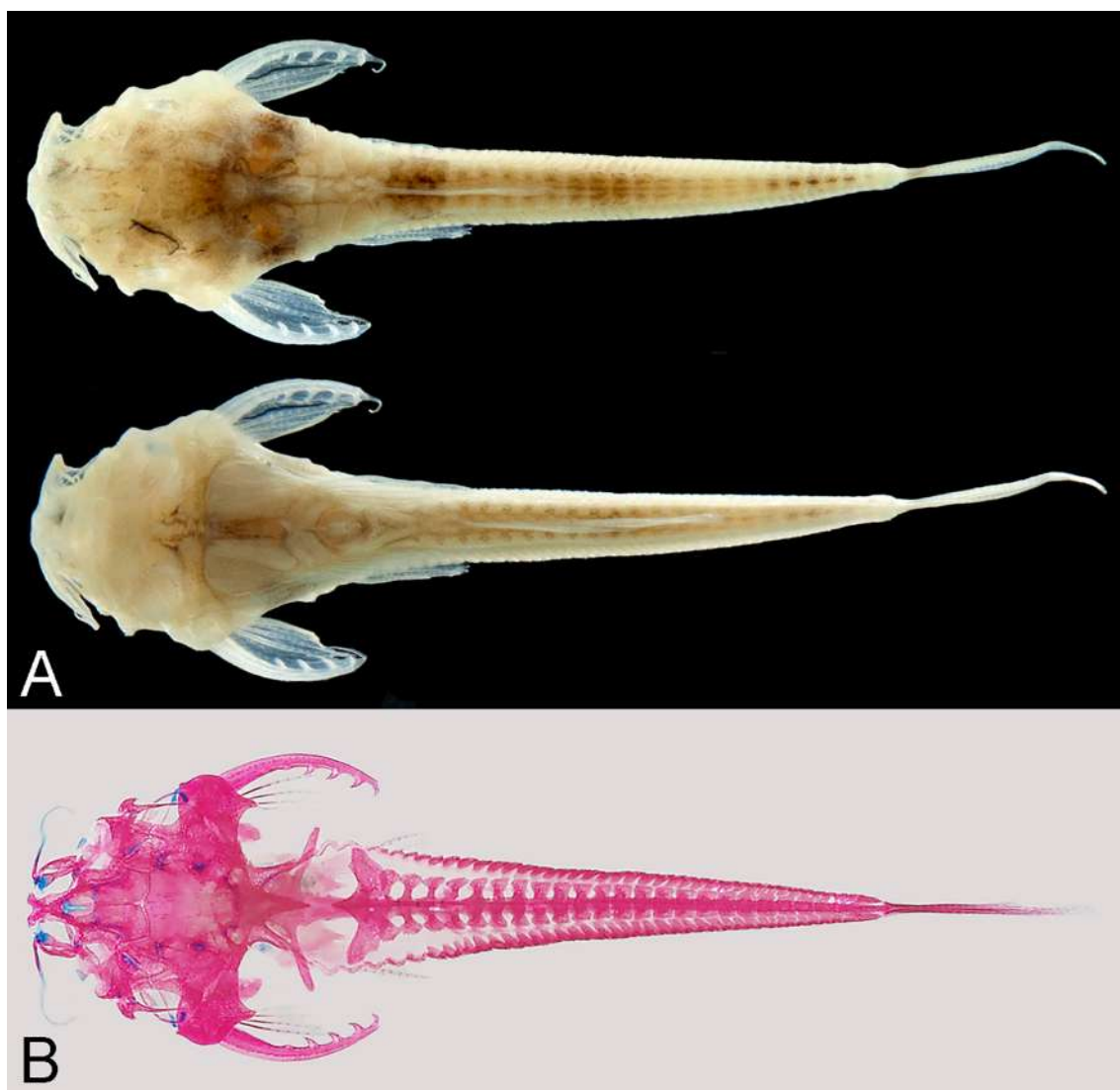


Fig. 12. Pictures of *Micromyzon akamai*. A. Dorsal (above) and ventral (below) views of ANSP 180358, 15.4 mm SL. B. Dorsal view of cleared and stained specimen of ANSP 180882 (photo: K. Luckenbill).

rio Tapajós, 02°06'S 54°0'W. MZUSP 57267, 8, 11-14 mm SL, Amazonas, rio Amazonas, just upstream mouth of rio Madeira, 03°19'S 58°50'W. MZUSP 115533, 1, 6 mm SL, Rondônia, rio Machado 12 km upstream mouth, 08°07'33"S 62°49'47"W MZUSP 115535, 1, 14 mm SL, Rondônia, rio Madeira in front of Humaitá, 07°30'56"S 63°00'39"W. MZUSP 115536, 1, 16 mm SL, Rondônia, rio Madeira just downstream from Santo Antonio hydroelectric power plant, 08°47'08"S 63°55'35"W. MZUSP 115537, 1, 10 mm SL, Rondônia, rio Madeira downstream Porto Velho in front of comunidade Cujubim, 08°34'55"S 64°44'56"W MZUSP 115544, 1, 7 mm SL, Rondônia, rio Madeira in front of Humaitá, 07°30'56"S 63°00'39".

ACKNOWLEDGEMENTS

For help in the fish collections or for lending valuable material for study we would like to thank M. Arce and M. Sabaj (ANSP), C. Dardia (CUMV); Caleb McMahan and S. Mochel (FMNH); L. Rapp Py-Daniel (INPA); O. Castillo (MCNG); A. Datovo, M. Gianetti, and O. Oyakawa (MZUSP); and F. Carvajal (UMSS). We thank J. Maisano and M. Colbert (UT Austin) for preparation of CT scans and K. Luckenbill (ANSP) for expert guidance in image editing with VGStudio Max software. Thanks to J. Chuctaya for help translating the abstract to Spanish. The first author (TPC) thanks to Conselho Nacional de Desenvolvimento Científico e Tecnológico (CNPq; process number 229355/2013-7) for a postdoctoral fellowship and CAPES for a PNPd fellowship. The computed tomography was supported by Fundação de Amparo à Pesquisa do Estado do Rio Grande do Sul - FAPERGS (2361-2551/14-7). Support for the exploratory field work in Venezuela that discovered the type specimens described herein came from the U.S. National Science Foundation to JGL and JNB: DEB 77-14439. For that work we acknowledge use of R/V Eastward operated by Duke University; the Duke National Oceanographic Facility was supported in 1978 and 1979 by NSF, CG-00005.

LITERATURE CITED

- Cardoso, A. R. 2008. Filogenia da família Aspredinidae Adams, 1854 e revisão taxonômica de Bunocephalinae Eigenmann & Eigenmann, 1888 (Teleostei: Siluriformes: Aspredinidae). Unpublished PhD dissertation, Pontifícia Universidade Católica do Rio Grande do Sul, 259 pp.
- Cardoso, A. R. 2010. *Bunocephalus erondinae*, a new species of banjo catfish from southern Brazil (Siluriformes: Aspredinidae). *Neotropical Ichthyology* 8:607-613.
- Carvalho T. P., A. R. Cardoso, J. P. Friel, and R. E. Reis. 2015. Two new species of the banjo catfish *Bunocephalus* Kner (Siluriformes: Aspredinidae) from the upper and middle rio São Francisco basins, Brazil. *Neotropical Ichthyology* 13:499-512.
- Carvalho T. P. and J. S. Albert. 2011. Redescription and Phylogenetic position of the enigmatic Neotropical electric fish *Iracema caiana* Triques (Gymnotiformes: Rhamphichthyidae) using x-ray computed tomography. *Neotropical Ichthyology* 9:457-469.
- Carvalho T. P., R. E. Reis and M. H. Sabaj. In press a. Description of a new blind and rare species of *Xylophius* (Siluriformes: Aspredinidae) from the Amazon basin using High-resolution Computed Tomography. *Copeia*.
- Carvalho T. P., R. E. Reis and J. P. Friel. In press b. A new species of the genus *Hoplomyzon* Myers (Siluriformes: Aspredinidae) from Lake Maracaibo tributaries, Venezuela: Osteological description using high-resolution computed microtomography of a miniature species. *Neotropical Ichthyology*.
- Dahdul, W. M., P. M. Mabee, J. G. Lundberg, P. E. Midford, J. P. Balhoff, H. Lapp, T. Vision, M. A. Haendel, and M. Westerfield. 2010. The teleost anatomy ontology: anatomical representation for the genomics age. *Systematic Biology* 50:369-683.
- Eschmeyer, W. N., and J. D. Fong. 2016. Species by Family/Subfamily. (<http://researcharchive.calacademy.org/research/ichthyology/catalog/SpeciesByFamily.asp>). Electronic version accessed 12 Sep 2016.
- Fernández-Yepéz, F. 1953. Algunas notas sobre los peces Asprediniformes con descripción de *Ernstichthys anduzei*, nuevo e interesante bunocephalido. *Novedades Científicas Museo Historia Natural La Salle Zoologia* 11:1-7.
- Friel, J. P. 1994. A phylogenetic study of the Neotropical banjo catfishes (Teleostei: Siluriformes: Aspredinidae). Unpublished PhD dissertation, Durham, Duke University, 256p.
- Friel, J. P. 1995. *Acanthobunocephalus nicoi*, a new genus and species of miniature banjo-catfish from the upper Orinoco and Casiquiare Rivers, Venezuela (Siluriformes: Aspredinidae). *Ichthyological Exploration of Freshwaters* 6:89-95
- Friel, J. P. 2003. Family Aspredinidae. In: Reis, R. E. S. O. Kullander and C. J. Ferraris Jr. (eds.). Check list of the freshwater fishes of South and Central America. Edipucers, Porto Alegre, pp. 261-267.
- Friel, J. P., and J. G. Lundberg. 1996. *Micromyzon akamai*, gen. et sp. nov., a small and eyeless banjo catfish (Siluriformes: Aspredinidae) from the river channels of the lower Amazon basin. *Copeia* 1996:641-648.

- Friel, J. P., and T. P. Carvalho. 2016. A new species of *Amaralia* Fowler (Siluriformes: Aspredinidae) from the Paraná-Paraguay River Basin. *Zootaxa* 4088:531–546.
- Jarduli, L. R., A. Claro-García, and O. A. Shibatta. 2014. Ichthyofauna of the rio Araguaia basin, states of Mato Grosso and Goiás, Brasil. *Check List* 10:483-515.
- Lundberg, J. G., K. R. Luckenbill, K. K. Subhash Babu, and H. H. Ng. 2014. A tomographic osteology of the taxonomically puzzling catfish *Kryptoglanis shajii* (Siluriformes, Siluroidei, *incertae sedis*): description and a first phylogenetic interpretation. *Proceedings of the Academy of Natural Sciences of Philadelphia* 163:1-41.
- Lundberg, J. P., and L. Rapp Py-Daniel. 1994. *Bathycetopsis oliveirai*, Gen. et Sp. Nov., a blind and depigmented catfish (Siluriformes: Cetopsidae) from the Brazilian Amazon. *Copeia* 1994:381-390.
- Maldonado-Ocampo, J.A., A. Ortega-Lara, J.S. Usma, G. Galvis, F.A. Villa-Navarro, L. Vasquez, S. Prada-Pedreiros, and C.A. Ardila R. 2005. Peces de los Andes de Colombia: guía de campo. 1. ed. Bogotá: Instituto de Investigación de Recursos Biológicos Alexander von Humboldt. 346 p.
- Mungall, C. J., C. Torniai, G. V. Gkoutos, S. E. Lewis, and M. A. Haendel. 2012. Uberon, an integrative multi-species anatomy ontology. *Genome Biology* 13:R5.
- Ohara, W. M., and J. Zuanon. 2013. Aspredinidae. In: Queiroz L. J., G. Torrente-Vilara, W. M. Ohara, T. H. S. Pires and J. Zuanon (eds.). *Peixes do rio Madeira*. São Paulo, Santo Antonio Energia, pp. 108-141.
- Parisi, B. M., and J. G. Lundberg, 2009. *Pimelabditus moli*, a new genus and new species of pimelodid catfish (Teleostei: Siluriformes) from the Maroni River basin of northeastern South America. *Notulae Naturae*, 480:1-11.
- de Pinna, M. C. C. 1996. A Phylogenetic analysis of the Asian catfish families Sisoridae, Akysidae, and Amblycipitidae, with a hypothesis on the relationships of the Neotropical Aspredinidae (Teleostei, Ostariophysii). *Fieldiana, Zoology*, 84:1-83.
- Rodiles-Hernández, R., D. A. Hendrickson, J. G. Lundberg, and J. M. Humphries. 2005. *Lacantunia enigmatica* (Teleostei: Siluriformes) a new and phylogenetically puzzling freshwater fish from Mesoamerica. *Zootaxa* 1000:1-24.
- Sabaj Pérez, M. H. 2009. Photographic atlas of fishes of Guiana shield. In: Vari R.P., C.J. Ferraris, A. Radosavljevic and V.A. Funk (eds.). *Checklist of the freshwater fishes of the Guiana Shield*. Washington D.C.: Bulletin of the Biological Society of Washington, op. 53-59.
- Sabaj, M. H. 2016. Standard symbolic codes for institutional resource collections in herpetology and ichthyology: an Online Reference. Version 6.5 (16 August 2016). Electronically accessible at <http://www.asih.org/>, American Society of Ichthyologists and Herpetologists, Washington, DC.
- Schaefer, S. A. 2003 Relationships of *Lithogenes villosus* Eigenmann, 1909 (Siluriformes, Loricariidae): evidence from high-resolution computed microtomography. *American Museum Novitates* 3401:1-55.
- Schaefer S. A., and L. Fernández. 2009. Redescription of the Pez Graso, *Rhizomichthys totae* (Trichomycteridae) of Lago Tota, Colombia, and aspects of cranial osteology revealed by microtomography. *Copeia* 2009:510-522.
- Schaefer S. A., S. H. Weitzman, and H. A. Britski. 1989. Review of the Neotropical catfish genus *Scoloplax* (Pisces: Loricarioidea: Scoloplacidae) with comments on reductive characters in phylogenetic analysis. *Proceedings of the Academy of Natural Sciences of Philadelphia* 141:181-211.
- Stewart, D. J. 1985. A review of the South American catfish tribe Hoplomyzontini (Pisces, Aspredinidae), with descriptions of a new species from Ecuador. *Fieldiana, Zoology* 25:1-19.
- Stewart, D. J., M. Ibarra, and R. Barriga-Salazar. 2002. Comparison of deep-river and adjacent sandy-beach fish assemblages in the Napo River basin, eastern Ecuador. *Copeia* 2002:333-343.
- Taphorn, D. C., and C. Marrero. 1990. *Hoplomyzon sexpapilostoma*, a new species of Venezuelan catfish (Pisces: Aspredinidae), comments on the Hoplomyzontini. *Fieldiana, Zoology* 61:1-9.
- Taylor, W. R., and G. C. Van Dyke. 1985. Revised procedures for staining and clearing small fishes and other vertebrates for bone and cartilage study. *Cybiurn* 9:107-119.
- Weitzman, S. H., and R. P. Vari. 1988. Miniaturization in South American freshwater fishes; an overview and discussion. *Proceedings of Biological Society of Washington* 101:444-465.

